JOURNAL OF AGRICULTURAL AND FOOD CHEMISTRY

ARTICLE

pubs.acs.org/JAFC

Scorpion Toxins Modify Phytopathogenic Fungus Physiology. A Possible Source of New Fungicides

Galax Joya,[†] Gina D'Suze,[*,†] Víctor Salazar,[‡] Arnaldo Rosales,[†] Carlos Sevcik,[†] Gonzalo Visbal,[§] André T. S. Ferreira,[#] and Jonas Perales[#]

[†]Laboratory on Cellular Neuropharmacology and [‡]Histology Service, Biophysics and Biochemistry Center, and [§]Laboratory of Natural Products, Chemistry Center, Instituto Venezolano de Investigaciones Científicas (IVIC), Caracas, Venezuela

[#]Laboratory of Toxinology, Oswaldo Cruz Foundation (FIOCRUZ), Rio de Janeiro, Brazil

ABSTRACT: Seven toxins (**F1**−**F7**) were purified from *Tityus discrepans* scorpion venom on a C18 HPLC column. The compounds were fungitoxic on *Macrophomina phaseolina*. The molecular masses of **F1**−**F7** were (Da) 1061.1, 7328.8, 7288.3, 7268.5, 7104.6, 6924.6, and 6823.3, respectively. It is not known if **F1** is a small peptide or some other kind of organic molecule. Compounds **F2**−**F7** were peptides. The most potent was **F7**, with a minimal inhibition concentration of 0.4 μg/μL and a concentration for 50% inhibition of 0.13 μg/μL. Fungal esterase activity was abolished by **F2**, **F3**, and **F5** and inhibited by 89, 60, 58, and 54% by **F4**, **F6**, **F7**, and **F1**, respectively. **F1**, **F2**, **F5**, and **F7** induced an increase on hyphae chitin wall and septum thickness. Peptides **F3**−**F6** induced efflux of the fluorescent dye Na−CoroNa Red complex from hyphae. Only **F5** and **F6** were inhibited by the prokaryote sodium channel blockers amiloride and mibefradil. Gas chromatography−mass spectrometry analysis suggested that **F1**, **F5**, **F6**, and **F7** altered sterol biosynthesis either by inhibiting ergosterol biosynthesis or by producing ergosterol analogues. The peptides affect *M. phaseolina* viability by three mechanisms: decreasing esterase activity, altering Na^+ membrane permeability, and altering wall sterol biosynthesis. It seems that interfering with sterol synthesis is an important mechanism behind the effect of the fungicideal toxins. However, the antifungal effects at short times are indicative of a direct esterase inhibition, which, with the increased membrane leakiness to Na^+, makes the fungus inviable.

KEYWORDS: *Macrophomina phaseolina*, fungicidal toxins, *Tityus discrepans* scorpion venom, esterase activity, Na^+ membrane permeability, fungus membrane sterols

INTRODUCTION

Phytopathogenic fungi cause 35% of worldwide crop loss.[1] *Macrophomina phaseolina* is a globally distributed Ascomycote able to infect a wide range of crops including soybean, corn, and common bean and a wide range of citrus. This fungus survives in soil or on infected plants as microesclerotium. It has become resistant to many chemical fungicides in current use. Thus, research on plant pathology focuses on new antifungal agents gentle to the environment. Scorpion venoms are a rich source of biodegradable peptides able to interact with cell membranes of living species from diverse taxa. Despite their structural similarity, they are highly varied in their primary structure, having six or eight structure-stabilizing Cys.[2] The variation in amino acid sequence accounts for the different biological activities produced by this venom; these include neurotoxins able to modulate membrane ionic channels (Na^+, K^+, Ca^{2+})[3] and disrupt cellular communication. Scorpion habitat and habits make them victims of saprophytic organisms such as bacteria and fungi. Some species, such as *Tityus discrepans*, spray their venom on their bodies to clean it from lichens, fungi, and bacteria. The presence of antimicrobial compounds in scorpion venom and hemolymph has been previously demonstrated.[4−10] The compounds protect scorpions against contamination when stinging and against environment hostility and generally serve as an innate mechanism of adaptive immunity.[11] *Tityus* is the genus most abundant in South America, and its species' venoms have been extensively studied. From their mass spectrometry studies, Pimenta and co-workers[12] reported up to 380 different components in *Tityus serrulatus*, and our group reported up to 205 different components in *T. discrepans*;[13] peptides with antifungal activities have not yet been reported in these venoms. Scorpion venom compounds could be useful as biodegradable fungicides and therefore could be of particular interest from an agrochemical perspective, enticing our interest to study *T. discrepans* venom as a source of antifungal peptides.

MATERIALS AND METHODS

Fungus Source. *M. phaseolina* was isolated from bean plants and taxonomically identified by Dr. Luis Subero from the Agronomy School, Central University of Venezuela (UCV), and by Dr. Maria Gonzalez from INIA-Ceniap. Fungi were maintained under sterile conditions and were grown on potato dextrose agar (PDA) plates for 3−7 days at 28 °C, under 12 h light/12 h darkness cycles. Once grown, a batch was stored at 4 °C until used, and another batch was maintained at 28 °C in up to five replicates. We used potato dextrose broth (PDB; HIMEDIA, Mumbai, India) (pH 5) in experiments for which liquid medium was required. In these cases, fungi were incubated at 28 °C without agitation in 1 mL of PDB, from 2 to 4 days, under 12 h light/12 h darkness cycles.

Received: February 9, 2011
Revised: April 19, 2011
Accepted: April 21, 2011
Published: April 21, 2011

Venom Source and Extraction. Adult *T. discrepans* scorpions were collected around Caracas (Venezuela) and kept in plastic boxes with water and food ad libitum. Adult specimens (≈200) were anesthetized once a month with CO_2 and milked for venom by electrical stimulation.[14] Venom was dissolved in double-distilled water and centrifuged at 15000*g* for 15 min at 5 °C. Protein content was estimated on the basis of absorbance at 280 nm, assuming that 1 mg/mL protein produces 1 unit of absorbance per unit path length. The supernatant was freeze-dried using a Savant Speed-Vac dryer (SC110, New York) and stored at −80 °C until used.

Venom Components Isolation. Venom was fractionated through an analytical reversed phase C18 column (250 × 10 mm, Vydac, Hesperia, CA) coupled on a high-performance liquid chromatograph (HPLC) with a photodiode array detector (Water Corp. 2695, 2996). Elution of venom components was performed at a flow rate of 1 mL/min using a linear gradient from solution A [0.12% trifluoroacetic acid (TFA) in water] to 60% solution B (0.10% TFA in acetonitrile) in 60 min and detected at a wavelength of 230 nm.[14] Fractions were manually collected and freeze-dried. Active fractions were further purified through the same column and under similar conditions but using a less steep linear gradient. **F1** was purified using a gradient from 0 to 20% solution B in 60 min. **F2**, **F3**, **F4**, **F5**, and **F6** were purified with a gradient from 15 to 40% solution B in 75 min, and **F7** was purified with a gradient from 25 to 50% solution B in 75 min. Purified components were manually collected, lyophilized, and kept at −80 °C until used. Subsequently, components were dissolved in distilled water, PDB, choline chloride, or phosphate-buffered saline (PBS) according to the activity to be evaluated. These components were used for determining the MIC and IC_{50} for mass spectrometry analysis and to study their effect on fungal esterase activity, morphology, membrane sodium ion flux, and fungal membrane lipid composition.

Mass Spectrometry (MS) Analysis. Tryptic digestion was performed with the method of Simpson.[15] C4 and C18 ZipTip micropipet tips were used for desalting the native and tryptic peptides, respectively. For MS analysis the peptides were cocrystallized with 0.3 μL of 10 mg/mL α-cyano-4-hydroxycinnamic acid solution in 0.1% (w/v) TFA−50% (v/v) acetonitrile directly on a matrix-assisted laser desorption/ionization (MALDI) target plate. Raw data for protein identification were obtained with a 4700 Proteomics Analyzer (Applied Biosystems, Foster City, CA). MS data were acquired in positive linear and reflectron mode, and MS/MS data were acquired only in positive and reflectron mode using a neodymium-doped yttrium aluminum garnet (Nd:YAG) laser with a 200- Hz repetition rate. Typically, 1000 shots were accumulated for spectra in linear mode mass ranges 700−4000 (low mass), 1000−15,000 (middle mass), and 8000−100,000 (high mass) and 1600 shots for reflectron MS mode (MS1), whereas 3000 shots were accumulated for spectra in MS/MS mode (MS2). Up to 10 of the most intense ion signals with signal-to-noise ratio above 20 were selected as precursors for tandem mass spectrometry (MS/MS) acquisition excluding common trypsin autolysis peaks and matrix ion signals. External calibration in MS mode was performed using a mixture of four peptides: des-Arg1-bradykinin (m/z 904.47), angiotensin I (m/z 1296.69), Glu1-fibrinopeptide B (m/z 1570.68), and ACTH (18−39) (m/z 2465.20). MS/MS spectra were externally calibrated using known fragment ion masses observed in the MS/MS spectrum of angiotensin I. MS/MS database searching was against the NCBInr databases using the Mascot software (www.matrixscience.com). The search parameters were as follows: two tryptic miss cleavages allowed, nonfixed modifications of methionine, tryptophan, histidine (oxidation), and cysteine (carbamidomethylation). The mass list files were generated from the raw (or native) MS data according to the following parameters using Data Explorer software (Applied Biosystems): for MS1, mass range, 900−4000; peak density, 15 peaks per 200 Da; signal-to-noise ratio, 20; minimum area, 100; maximum peaks per spot, 60; for MS2, mass range, 60 Da until precursor mass; peak density, 55 peaks per 200 Da; signal-to-noise ratio, 2; minimum area, 10; and maximum peaks per precursor, 200. The MASCOT score was considered to be significant if over 40 for protein ion score.

Fungus Growth Conditions. *M. phaseolina* stock solution was made by homogenizing a portion of mycelium in 1 mL of PDB, pH 5. Spores and mycelial fragments were quantified in a Neubauer chamber. Four fungus dilutions in PDB were made, 2×10^4, 30×10^4, 100×10^4, or 200×10^4 cells/mL, to determine the optimal growth concentration. Fungal growth curves were made by placing 100 μL/well in polystyrene microplates of 96 wells (Nunc, Denmark) and incubated under 100 rpm agitation in a moist chamber at 28 °C, with 12 h light/12 h darkness cycles.[16,17] Fungal growth was monitored by absorbance at 405 nm (Multiskan 352, ThermoLabsystems Spectrometer, Finland), every 3 h for 100 h.[16,17]

Assaying Effects of Whole Venom and Isolated Toxins on Fungal Growth. *M. phaseolina* (2×10^4 cells/mL) cultured in PDB, pH 5, in a 96-well plate were exposed after 12 h of culture (6 h before exponential growth phase under control condition) to whole venom (0.5, 1, and 2 μg/μL PDB) or HPLC isolated fractions (0.1 and 1 μg/μL PDB). Fungi were incubated as previously described. The control group was exposed to PDB only.

Determining the Inhibitory Effects of HPLC-Isolated Toxins on *M. phaseolina*. The inhibitory potency of the toxins was expressed as the minimal inhibitory concentration (MIC) and the inhibitory concentration 50 (IC_{50}). The MIC is the lowest concentration causing 100% fungus growth inhibition, and the IC_{50} is the concentration inhibiting 50% fungus growth. MIC and IC_{50} were determined after finding the time needed by the fungus to reach its stationary phase and the time needed to reach 50% fungus growth under control conditions. MIC and IC_{50} of the active compounds were determined following the microdilution method to study antifungal suceptibility of filamentous fungi.[18] *M. phaseolina* (2×10^4 cells/mL) was cultured in PDB, pH 5, in a 96-well plate under the same conditions described above and, after 12 h of growth, exposed to the active toxins (decreasing concentrations series 20×). Fungal growth was monitored in a spectrophotometer at 405 nm every 6 h for 60 h to determine MIC and for 39 h for IC_{50}. The control group was exposed only to PDB.

Assaying Effects of Purified Toxins on *M. phaseolina* Viability. *M. phaseolina* microcultures were made as follows: PDA plate sections arranged in 1 × 1 cm slides were inoculated with the fungus, covered with a coverslip, and incubated in a moist chamber at 28 °C, with light for a period of 2−4 days. The mycelium attached to the coverslip was then exposed to 300 μL of active compounds at its MIC in PBS. The negative control was exposed to 300 μL of PBS and the positive control to 300 μL of fluconazole (100 μg/mL). Microcultures were incubated for 1 h, washed three times with PBS, and then incubated during 5 min with 300 μL of a solution of 0.01% FDA (Sigma, St. Louis, MO) in PBS, pH 7, protected from light.[19] All experiments were carried out under controlled conditions of pH and temperature, because changes in pH and temperature affect enzyme activity.[20] After this time, microcultures were washed three times with PBS, placed on a Neubauer chamber with 10 μL of PBS, observed by epifluorescence microscopy (Eclipse E600 microscope, Nikon, Tokyo, Japan) with a 40× objective, a B-2A filter cube, and an attenuating ND4 filter, and digitally photographed with a Coolpix 8700 camera (Nikon).

Assaying Effects of Purified Toxins on *M. phaseolina* Morphology. Fungus morphology after exposure to active compounds was studied with calcofluor white (0.01%) (Fluorescent Brightener 28, Sigma-Aldrich, St. Louis, MO) following the protocol of Monheit and co-workers[21] with some modifications. *M. phaseolina* (2×10^4 cells/mL) was cultured in PDB (pH 5) in a 96-well plate and incubated after 12 h with active toxins (at its IC_{50}) as explained before. The control group was exposed to PDB. A fungus group was

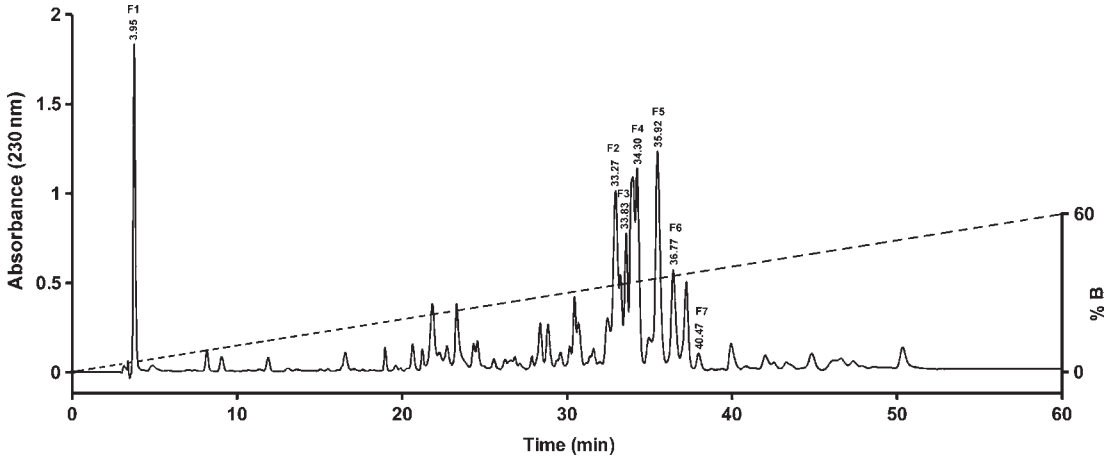

Figure 1. Venom fractionation: chromatographic profile of *T. discrepans* venom fractionated on an analytical reversed phase C18 column on a HPLC at a flow rate of 1 mL/min using a linear gradient from solution A [0.12% trifluoroacetic acid (TFA) in water] to 60% solution B (0.10% TFA in acetonitrile) in 60 min and detected at a wavelength of 230 nm. Active fungicidal toxins are identified as **F1**−**F7** with their respective retention times.

incubated for 18 h and another group for 36 h. The fungal content of each well was removed and individually placed in Eppendorf tubes with 70% ethanol and centrifuged at 15000*g* for 2 min. Supernatants were discarded, and cells were washed with 1 mL of deionized water; this step was repeated three times. Fungus groups incubated for 18 h were resuspended in 50 μL of deionized water, whereas fungus groups incubated during 36 h were resuspended with 100 μL of deionized water. Fifty microliters of each fungal suspension were dried on slides, stained with 25 μL of calcofluor (0.01%), and covered with a coverslip. Morphological changes were observed by epifluorescence using a Nikon UV2A filter cube.

Assaying Effects of Active Toxins on Fungus Na^+ Membrane Permeability. Na^+ efflux was monitored in *M. phaseolina* microcultures exposed to the toxins in a manner similar to that of Diaz et al.[10] With a coverslip-attached mycelium atop a Neubauer chamber and using a Hamilton microsyringe with a catheter on the tip, 5 μL of sterile choline chloride solution (pH 7) was added to the chamber. The mycelium was then washed and loaded with 1 μM CoroNa Red (Molecular Probes, Eugene, OR) for 10 min at 37 °C. CoroNa Red is a cationic dye that can be loaded into cells as a fluorescent indicator for Na^+.[22,23] Fungal mycelium was washed three times with sterile choline chloride (0.15 M), placed on the chamber with 5 μL of sterile choline chloride (0.15 M), and photomicrographed before and 0.5, 1, 5, and 10 min after the additionn of the toxins at concentrations 10 times their IC_{50}. The control group was exposed to 0.15 M sterile choline chloride.

To evaluate the effect of the toxins on Na^+ channels, CoroNa Red loaded fungi were incubated with tetrodotoxin (10 μM), amiloride (10 μM), or mibefradil (25 μM) for 10 min at 37 °C in darkness and then exposed to the toxins (at concentrations 10 times their IC_{50}) mixed with the concentration of inhibitor under test. CoroNa Red loaded fungi exposed to sterile choline chloride (0.15 M) were used as control.

Microscopic Observation and Integrated Optical Density Measurements. Observation and imaging of fluorescent fungi were done as described by Iwamoto and Allen[24] with some modifications. The observations were carried out using a Nikon G-2A filter cube for CoroNa Red. Micrographies were also taken in the chamber with venom, but in the absence of fungi, using the same photomicrography conditions as in the presence of fungi; the background level was then subtracted from the mycelium pictures. Fluorescence was measured from the pictures as integrated optical density (IOD) inside the mycelium and in its neighboring medium using the ImageJ 1.41 computer program (http://rsbweb.nih.gov/ij/).[25] The IOD was measured (before and 0.5, 1, 5, and 10 min after the addition of venom or isolated toxins) in 14 randomly selected areas, 7 in the central cytoplasmic hyphae region and 7 at the immediate vicinity of the same hyphae. The IOD of these areas was automatically calculated with ImageJ and represents the average of red, green, and blue color values (RGB) of the analyzed area, expressed in optical units per surface area. A selection square of 20 × 20 pixels was used to measure IOD; the selection square occupied almost entirely the diameter of the hyphae. The same procedure was applied to obtain the background optical density in the fungus-free pictures as explained above. A single area was enough for background subtraction, because the background was constant in each photomicrograph. The linearity of the measurement corresponding to the actual fluorescence under the experimental conditions was verified by measuring IOD excited by different intensities of UV through the ND filters.[24]

Effect of Purified Toxins on Fungal Membrane Sterol Composition. *M. phaseolina* was cultured as indicated before and incubated per triplicate for 12 h with the toxins at their IC_{50} as indicated previously. After 60 h, fungal material from each well was transferred to Eppendorf tubes containing 1 mL of PBS, pH 7, and centrifuged at 20800*g* for 5 min at 4 °C. Pellets were washed three times with PBS, homogenized, and resuspended independently with chloroform/methanol 2:1 (v/v), to make a final volume of 1000 μL, and kept at 4 °C for 48 h. Each colony was independently filtered through a piece of cotton wool placed in a glass funnel to separate unwanted solids. Lipid extracts from each sample were dried in a rotary evaporator.[26] Neutral and polar lipids were separated following the Visbal and San-Blas[27] method. A silicic acid (100 mesh) chromatography column was activated for 12 h at 100 °C, packed inside a glass column (80 × 1.5 cm), resuspended in chloroform maintaining a density of 5 g/mL, and equilibrated with 4 chloroform volumes. Fungal lipid samples were resuspended with 1 mL of chloroform, placed independently on the column, eluted with 5 additional chloroform volumes, dried in a rotary evaporator, and preserved at 4 °C until analyzed.

Membrane sterols were analyzed by gas chromatography−mass spectrometry (Agilent, model 6890/5973). Chromatography grade cholesterol, ergosterol, and pregnelonone (1 mg/mL) dissolved in chloroform were used as standards. Control and experimental samples were resuspended in 400 μL of chloroform and passed in duplicate through an HP Ultra-2 capillary column (30 m × 0.20 μm) cross-linked with phenyl-methyl silicone (5%) as stationary phase. The temperature program was developed in 41 min as follows: an initial temperature 50 °C for 1 min, raised to 280 °C at a rate of 25 °C/min and then to 300 °C at a rate of 1 °C/min. The injector was set in splitless mode for 1 min and then in split mode. High-purity helium was used as carrier at a

Table 1. Mass Spectrometry Results[a]

					M_r		
fraction	TM	AM	SC	PM	theor	exptl	error (ppm)
F1		1060.1					
F2	7298.46	7328.85	15	1	1345.5850	1345.5390	4.18
F3	7288.33	7279.45	17	3	1428.7084	1428.6489	41.64
					1556.7986	1556.7439	35.20
					1300.6026	1300.5539	37.44
F4	7288.33	7268.48	17	3	1300.6317	1300.5539	59.82
					1428.7343	1428.6489	59.77
					1556.8313	1556.7439	56.20
F5	7118.15	7104.61	50	3	1075.5458	1075.4974	27.57
					1709.7659	1709.6714	55.27
					2447.0132	2447.0132	33.02
F6	6927.89	6924.61	26	2	2447.0825	2447.0132	28.32
					2575.1851	2575.1082	29.90
F7	6835.99	6823.28	36	2	1253.7732	1253.7343	31.03
					2635.1182	2635.0348	31.68

fraction	IS	PIS	identified peptide sequence	GenBank ID	protein description
F1					no identification
F2	22	22	KGTYCADECSR + 2 CarMethCys	gi|71276985	putative neurotoxin Td11 precursor (*T. discrepans*)
F3	43	133	GTFCAETCSLR + 2 CarMethCys	gi|71276977	putative neurotoxin Td3 precursor (*T. discrepans*)
	71		KGTFCAETCSLR + 2 CarMethCys		
	21		KGTFCAETCSLRK + 2 CarMethCys		
F4	65	99	GTFCAETCSLR + 2 CarMethCys	gi|71276977	putative neurotoxin Td3 precursor (*T. discrepans*)
	30		KGTFCAETCSLR + 2 CarMethCys		
	6		KGTFCAETCSLRK + 2 CarMethCys		
F5	92	178	YSCFWGSSTWCNR + 2 CarMethCys	gi|115311309	ardiscretin precursor (*T. discrepans*)
	55		IFDYYNNK		
	32		GSSGYCAWPACWCYG + 3 CarMethCys		
F6	37	128	GSSGYCAWPACWCYGLPDNVK + 3 CarMethCys	gi|294956473	bactridin-1 (*T. discrepans*)
	93		KGSSGYCAWPACWCYGLPDNVK + 3 CarMethCys		
F7	51	149	LVTLIPNDTLR	gi|93115187	TdiβKTx-like (*T. discrepans*)
	99		TQFGCPAYEGYCMNHCQDIER + 3 CarMethCys		

[a] TM, theoretical mass (mature chain); AM, experimental average mass (linear mode); SC, sequence coverage (%); PM, peptides matched; CarMethCys, carbamidomethyl cysteine; IS, ion score; PIS, protein ion score. All masses are in Da. MSMS reflectron mode used for all fractions. Identity or extensive homology was >10 in all cases except **F1** ($P < 0.05$). Other details in the text of the paper.

constant flow of 0.5 mL/min. Free sterol electron impact mass spectra (EI) (70 eV) provided structural information.[27]

Statistical Analysis. The data were analyzed using nonparametric statistics; data are presented as medians and their 95% confidence intervals calculated with the Hodges and Lehman procedure.[28] Multiple sample comparisons were done with the nonparametric Kruskall and Wallis analysis of variance.[28] Differences between treatments were considered to be significant if the probability that the null hypothesis was true was $\leq 5\%$ ($P \leq 0.05$).

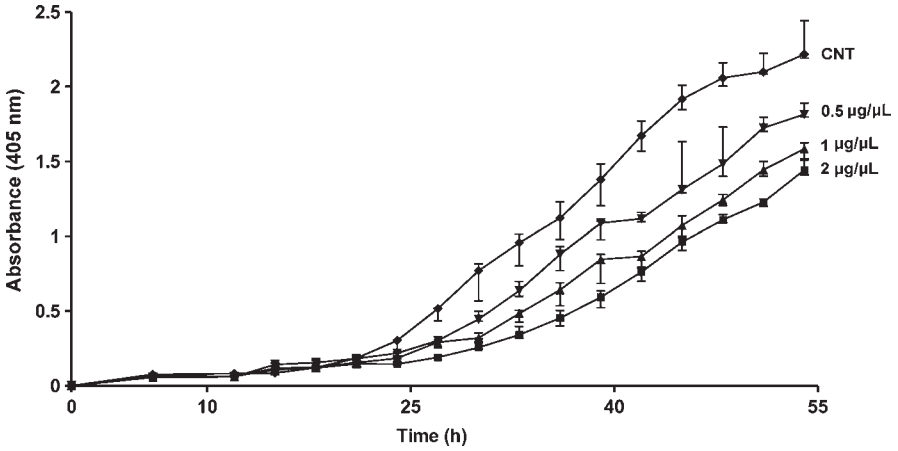

Figure 2. Effect of whole venom on fungal growth. *M. phaseolina* (2×10^4 cells/mL) cultured in PDB in a 96-well plate was exposed after 12 h (6 h before exponential fungal growth phase under control condition) to whole venom (0.5, 1, and 2 μg/μL PDB). Fungi were incubated as described under Materials and Methods. The control group was exposed to PDB only. Results are expressed as medians and their 95% confidence intervals, $n = 4$.

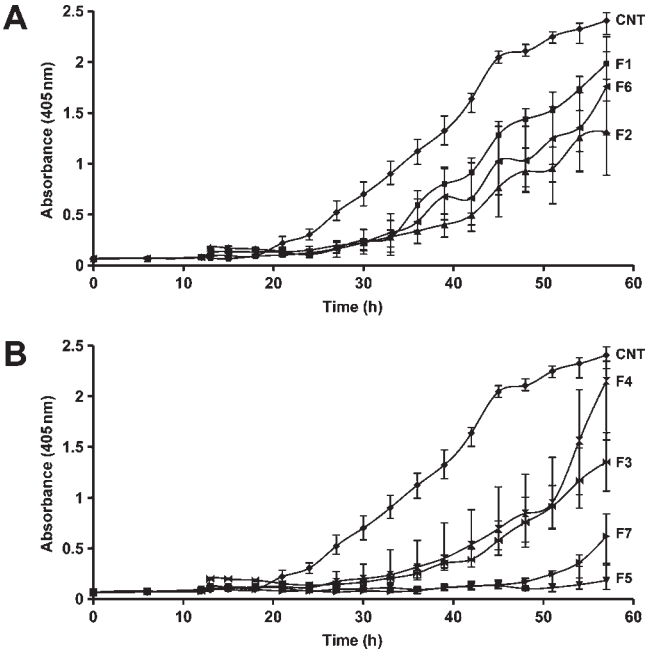

Figure 3. Effect of fungicidal toxins on fungal growth. Details as in Figure 2, $n = 6$.

RESULTS

Purification of Active Toxins. *T. discrepans* venom was separated into approximately 65 fractions (Figure 1), but only 7 (labeled with their retention times) inhibited fungus growth. Active antifungal compounds were named **F1**, **F2**, **F3**, **F4**, **F5**, **F6**, and **F7** and eluted at 3.95, 33.27, 33.83, 34.30, 35.92, 36.77, and 40.47 min, respectively. After successive rechromatographies through the same column, symmetric single peaks were obtained (data not shown) and were used for MS analysis. Table 1 shows that the approach used in the MS analysis yielded six positive identifications of the seven toxins studied; only **F1** remained unidentified. The molecular masses (Da) of the purified active components were **F1**, 1060.1; **F2**, 7328.9; **F3**, 7288.3; **F4**, 7268.5; **F5**, 7104.6; **F6**, 6924.6; and **F7**, 6823.3 (Table 1).

Table 2. Minimal Inhibition Concentration (MIC) and Inhibition Concentration 50 (IC_{50}) of HPLC Isolated Active Fractions[a]

toxin	MIC (μg/μL)	IC_{50} (μg/μL)
F1	4 (2, 4)	2 (1, 2)
F2	3 (2, 4)	1.5 (1.0, 2.0)
F3	3 (2, 4)	1.5 (1.0, 2.0)
F4	6 (4.5, 6)	3 (2.3, 3)
F5	2 (1.5, 2)	1 (0.9, 1)
F6	2.9 (1.8, 4)	1 (0.8, 1)
F7	0.4 (0.2, 0.5)	0.13 (0.07, 0.13)

[a] Results are expressed as median and their 90% confidence interval (between parentheses), $n = 3$.

Effect of Whole Venom and Isolated Toxins on Fungal Growth. *M. phaseolina* growth curves were determined in 12 experiments at 4 different fungus concentrations (not shown). One hundred microliters of medium sufficed to determine a curve in the 96-well microplate cultures. Latency, exponential, and stationary phases depended on fungus concentration; latency and exponential growth phase shortened when fungus concentration increased. A 2×10^4 cells/mL concentration was used in all experiments.

T. discrepans whole venom inhibited *M. phaseolina* growth. Higher venom concentration induced a greater inhibition of fungal growth (18.1, 28.5, and 35%, respectively) (Figure 2). A delay in the onset of exponential growth phase was observed after exposure to active toxins (Figure 3). Fungi exposed to **F1** began their exponential phase approximately 15 h after the controls, whereas those exposed to **F7** started approximately 30 h after the controls. Fungi exposed to **F5** did not reach exponential phase. Fungi exposed to **F1**, **F2**, and **F6** developed growth curves in wavy form (Figure 3A).

Minimal Inhibitory Concentration (MIC) and Inhibitory Concentration 50 (IC_{50}) of Active Toxins. The MIC values of **F1**, **F2**, **F3**, **F4**, **F5**, **F6**, and **F7** on *M. phaseolina* showed their ability to inhibit completely fungus growth at concentrations of 4, 3, 3, 6, 2, 2.9, and 0.4 μg/μL, respectively (Table 2). The IC_{50} values of the toxins were (μg/μL) **F1**, 2; **F2**, 1.5; **F3**, 1.5; **F4**, 3; **F5**, 1; **F6**, 1; and **F7**, 0.13 (Table 2). On the basis of their MIC

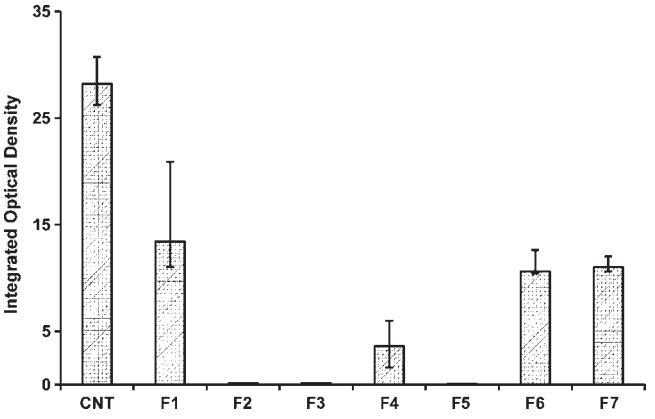

Figure 4. Effect of fungicidal toxins on fungal viability. *M. phaseolina* microcultures attached to a coverslip were exposed to 300 μL of active compound at its MIC dissolved in PBS and incubated for 1 h, washed three times with PBS, then incubated during 5 min with 300 μL of a solution of 0.01% FDA in phosphate-buffered saline protected from light, then washed three times with PBS, placed on a Neubauer chamber with 10 μL of PBS, and observed in a fluorescence microscope; hyphae were digitally photographed. The negative control was exposed to 300 μL of PBS and the positive control to 300 μL of fluconazole (100 μg/mL). Results are expressed as medians and their 95% confidence intervals, $n = 12$.

and IC_{50} on *M. phaseolina*, the antifungal potency of the active toxins was **F7** > **F5** > **F6** > **F3** > **F2** > **F1** > **F4**.

Effect of Active Toxins on *M. phaseolina* Viability. All toxins at their MIC inhibited fungal esterase activity. Figure 4 shows that after 1 h of exposure **F2**, **F3**, and **F5** inhibited completely esterase activity on *M. phaseolina*. The effects of **F1**, **F4**, **F6**, and **F7** were lower; however, they were able to inhibit esterase activity in 54, 89, 60, and 58%, respectively, compared to controls. The inhibition of fungal esterase activity was used as a measure of hyphae viability.

Effect of Active Toxins on *M. phaseolina* Morphology. Figure 5 contains photomicrographs of calcofluor white stained *M. phaseolina* exposed to active toxins at their IC_{50} for 36 h. This figure shows that fungi exposed to **F1**, **F2**, **F5**, and **F7** were more intensely stained than controls, suggesting a rise in hyphae chitin production. The toxins induced a chitin increase along the hyphae; **F1** and **F2** were more potent at inducing this effect. Under the action of **F2** and **F7** fungi experienced a considerable increase of septum thickness.

Effect of Active Toxins on *M. phaseolina* Membrane Na^+ Permeability. Changes on fungal sodium efflux were measured as the integrated optical density (IOD) at 0, 0.5, 1, 5, and 10 min after exposure to active toxins. Figure 6 shows that only **F3**, **F4**, **F5**, and **F6** induced changes on fungus membrane permeability to sodium ions. The Na−CoroNa Red complex efflux was observed as a decrease in fungal intracellular fluorescence (Figure 6A,B) with a simultaneous increase in fluorescence at the hyphae neighborhood (Figure 6C,D) during the first minute. Ten minutes after exposure of fungi to active toxins, most of its intracellular fluorescence leaked out and the band of fluorescence at the extracellular hyphae neighborhood was broad; dilution into the external buffer slowly faded the external fluorescence. Changes on *M. phaseolina* Na^+ membrane permeability induced by **F5** and **F6** were inhibited by a preincubation with the prokaryote sodium channel blockers amiloride (10 μM) and mibefradil (25 μM) (Figure 6B,D).

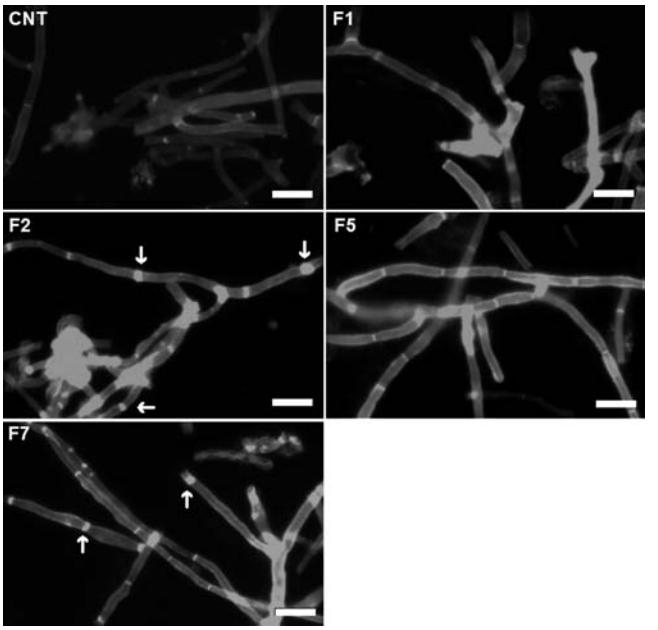

Figure 5. Effect of active compounds on fungal morphology. *M. phaseolina* (2×10^4 cells/mL) was cultured in PDB in a 96-well plate and incubated after 12 h to active toxins (at their IC_{50}) under the same conditions set out under Materials and Methods. The fungal content of each well was removed and washed with 70% ethanol and then with deionized water. Fungi were dried on slides and stained with calcofluor (0.01%). Morphological changes were observed with an epifluorescence microscope and digitally photographed. The control group was exposed to PDB. Results are expressed as medians and their 95% confidence intervals, $n = 4$. Calibration bars = 5 μm.

Effect of Active Toxins on *M. phaseolina* Membrane Sterol Composition. Only **F1**, **F5**, **F6**, and **F7** induced changes on fungal membrane sterol composition. As shown in Table 3, *M. phaseolina* membrane is composed by 100% ergosterol (ergosta-5,7,22-trien-3β-ol). The synthesis of membrane ergosterol was 51% blocked by exposing hyphae to **F5**, this peptide induced the accumulation of squalene.

Fungus incubation with **F1**, **F6**, and **F7** induced changes in sterol membrane composition, where the synthesis of ergosterol is replaced by desmosterol, β-sitosterol, or 22,23-dihydrostigmasterol. Exposure to these toxins induced the accumulation of some metabolites normally not produced by fungus under control conditions. **F1** changed 100% ergosterol membrane composition as 23% ergosterol, 39.1% desmosterol, and 41.8% β-sitosterol; however, exposure to **F6** induced the accumulation of 22,23-dihydrostigmasterol. Fungi exposed to **F7** replaced ergosterol with β-sitosterol.

DISCUSSION

We have shown that *T. discrepans* venom inhibits *M. phaseolina* growth and that this inhibition is concentration dependent. A simple microculture technique to monitor fungal growth with a microplate reader was found to be highly reproducible and sensitive.

Venom components with antifungal qualities were isolated by following their biological activity. Previous HPLC studies of *T. discrepans* venom on C18 columns[13] have shown that peaks eluting at similar retention times are clusters of compounds with similar size and activity. Compounds eluting during the first

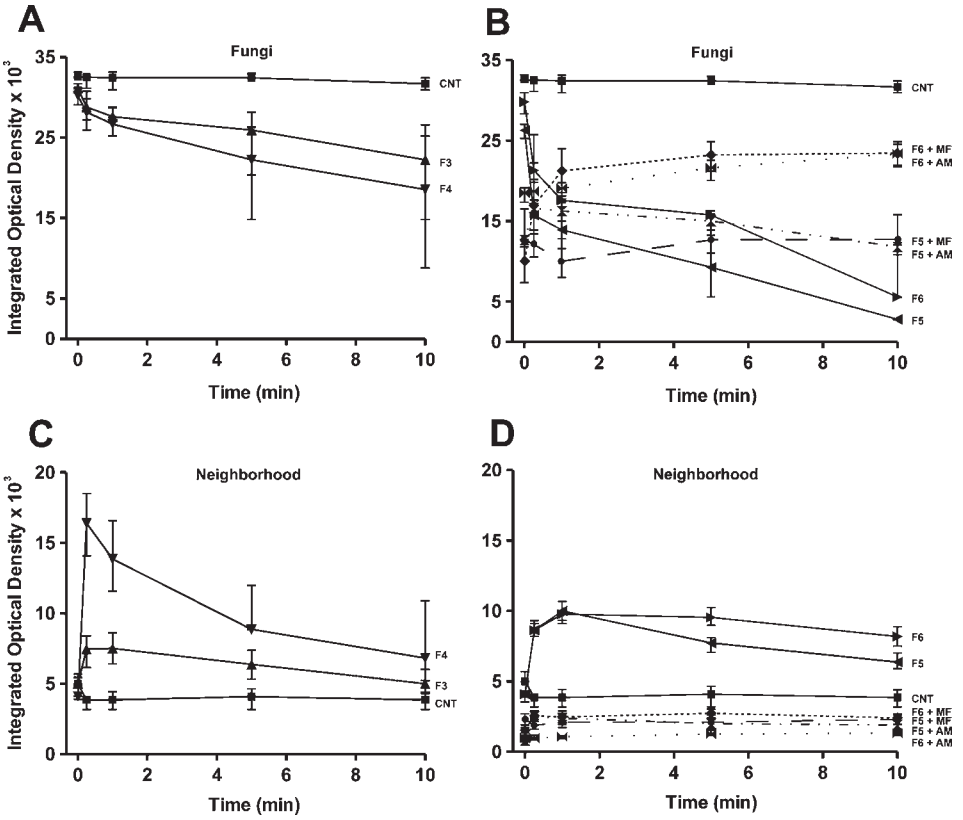

Figure 6. Effect of toxins on fungal Na^+ membrane permeability. *M. phaseolina* microcultures were made as described under Materials and Methods. The mycelia were then attached to a coverslip, washed, and loaded with 1 μM CoroNa Red for 10 min at 37 °C, washed three times with sterile choline chloride (0.15 M), placed under the microscope, and photographed before and 0.5, 1, 5, and 10 min after addition of the toxins at concentrations 10 times their IC_{50}. The control group was exposed to 0.15 M sterile choline chloride. Fluorescence was measured as integrated optical density (IOD) inside the mycelium and its neighboring medium from the photomicrographies. To evaluate the effect of the purified toxins on Na^+ channels, CoroNa Red loaded fungi were incubated with amiloride (AM) or mibefradil (MF) for 10 min at 37 °C in darkness and then exposed to toxins (at 10 times their IC_{50}) with the concentration of inhibitor under test. CoroNa Red loaded fungi exposed to sterile choline chloride (0.15 M) were used as control. Results are expressed as medians and their 95% confidence intervals, $n = 7$.

Table 3. Percent Sterol Composition of *M. phaseolina* Membranes Determined in Control Condition and after Exposure to Four Isolated Scorpion Toxins[a]

sterol	control	F1	F5	F6	F7
ergosterol	100	23	48.9	0	0
desmosterol	0	39.1	0	0	0
β-sitosterol	0	41.8	0	0	100
squalene	0	0	51.1	0	0
22,23-dihydrostigmasterol	0	0	0	100	0

[a] Control group was exposed to PDB. Other details in the text of the paper.

10 min have masses between 200 and 2000 Da; among these are toxins having inhibitory amidolitic activity of factor Xa and inhibitory plasmin activity.[29] Toxins eluting between 10 and 30 min have masses between 3 and 5 kDa; in this range eluted toxins with activity on membrane potassium channels.[13,14,30] Compounds eluting between 30 and 40 min have masses ranging from 5 to 8 kDa; this range includes toxins able to modulate membrane sodium channels.[10,13,31,32] The less hydrophilic proteins with high molecular weights elute at times >40 min; the latter include a curarizing peptide TdFI[33] and enzymes such as serino- and metalloproteinases[34] and other compounds with poorly understood functions. Of 65 isolated peaks only 7 inhibited *M. phaseolina*.

The MS analysis resulted in six positive identifications of seven toxins studied; only **F1** remains unidentified. **F1** produced no amino acids under tryptic digestion. We did not do ESI-MS/MS analyses or attempt Edman sequencing of **F1**. So, we do not know if it is a small peptide or some kind of other organic molecule. All of the compounds, except **F1**, have masses between 6823.3 and 7328.8 Da, typical of scorpion toxins acting on sodium channels.[3,32] **F5**'s mass matched that of ardiscretin, an arthropod selective sodium channel toxin.[32] Moreover, the two tryptic peptide sequences from **F5** matched perfectly with part of the ardiscretin sequence, suggesting strongly that **F5** is ardiscretin. The tryptic peptide sequence from **F6** matched partially both ardiscretin and bactridin 1 sequences.[10,32] Still, **F6**'s molecular mass was the same as that of bactridin 1, suggesting that **F6** may be bactridin 1.[10] **F5** and **F6** are proteins able to change the fungal sodium ion membrane permeability. Amino acid sequences of **F2** tryptic peptides allowed the identification of this toxin as a putative neurotoxin named Td11,[35] and the tryptic peptide sequences of **F3** and **F4** matched another putative neurotoxin named Td3.[35] The effects of Td3 and Td11 have not yet been studied.[35] **F7**'s mass matched the molecular weight of TdiβKTx,[36,37] the effects of which are also unknown, but which

was classified as a β-KTx-like peptide on the basis of its nucleotide and amino acid sequences. Another β-KTx-like peptide was found to be an antimicrobial and antiparasitic agent.[7]

The isolated compounds showed a potent inhibitory effect on *M. phaseolina* viability monitored using fluorescein diacetate (3′,6′-diacetylfluorescein, FDA), which is a fluorescein conjugated to acetate radicals. FDA is hydrolyzed by both free enzymes and membrane-bound enzymes,[38] releasing fluorescein. The enzymes responsible for FDA hydrolysis are involved in tissue decomposition and are found among the major decomposers such as bacteria and fungi. The use of fluorescein esters to measure enzyme activity was described by Kramer and Guilbault,[39] and Dittmer and Weltzien,[19] working with *Sclerotinia trifoliorum*, established the method as one to determine *Sclerotia* viability. We observed that **F2**, **F3**, and **F5** inhibited completely *M. phaseolina* esterase activity, whereas **F4** induced 80% inhibition and **F1**, **F6**, and **F7** inhibited only 60%. Peptides **F2**, **F3**, and **F5** seem to be fungicidal, whereas **F1**, **F4**, **F6**, and **F7** decreased fungus viability only partially, suggesting that these fractions are fungicidal; still, longer incubation times are required to ascertain this conclusion.[40]

M. phaseolina stained with calcofluor white, a dye for chitin and its derivatives, underwent gross structural changes after exposure to **F1**, **F2**, **F5**, and **F7**. These toxins induced chitin increase along the hyphae; **F1** and **F2** were the most potent compounds to induce these changes. Fungi under the action of **F2** and **F7** showed a considerable enhancement of septum thickness. Increments in chitin may be due to activation of chitin synthases. There are no chitin synthase genes known in *M. phaseolina*, but they are known to exist in fungi such as *Saccharomyces cerevisiae* and *Candida albicans*.[41] Another explanation for chitin increases could be that venom compounds inhibited chitinase activity, resulting in a chitin deposition enhancement. Augmented chitin deposition may be a defense mechanism.

Electrical excitability in fungi has long been known,[42,43] yet little is known about the presence of membrane ion channels in fungi. Mechanosensitive channels have been described in *S. cerevisiae*. These channels have a very poor selectivity, preferring cations over anions.[41] K^+ and Cl^- conductances with little discrimination between cations have been described in *Schizosaccharomyces pombe*.[44] Also, a Ca^{2+} conductance has been reported in *Uromyces appendiculatus* protoplasts;[45] it was suggested that this conductance triggers fungus differentiation.[46] Scant literature exists about Ca^{2+}, K^+, NH_4^+, and Cl^- channels in fungi.[47,48] We are not aware of any evidence on fungal membrane Na^+ channels, but their existence cannot be ruled out, especially if channels in fungi are not too selective. The NaChBact is a sodium channel described in *Bacillus hallodurans* with a physiology different from eukaryote Na^+ channels.[49] **F2**, **F3**, **F4**, **F5**, and **F6** eluted at times at which sodium channel toxins do, and their masses are in the range for known scorpion venom sodium toxins. Furthermore, as describe above, **F5** and **F6** molecular masses match the molecular masses of ardiscretin and bactridin 1, respectively. Ardiscretin is a toxin able to induce changes on arthropod sodium channels permeability,[32] and bactridin 1 induces changes on bacteria membrane sodium permeability.[10] All of these coincidences determined our study on hyphae Na^+ efflux. *M. phaseolina* exposure to **F3**, **F4**, **F5**, and **F6** resulted in a decrease of the intracellular Na−CoroNa Red fluorescence simultaneously with an enhancement of fluorescence at the hyphae neighborhood. The efflux of Na−CoroNa Red began immediately after exposure to the toxins ($\approx$15 s); 10 min later the hyphae had lost most of their intracellular fluorescence. These changes may be indicative of alterations in sodium ion membrane permeability. Only the effects of **F5** and **F6** were inhibited by amiloride (10 μM) and mibefradil (25 μM), suggesting that the effect occurs via fungal sodium channels. The effect of these compounds on Na−CoroNa Red efflux in *M. phaseolina* membrane is quite complex and requires further study to reach conclusions about the possible presence of sodium ion channels in this fungus. Shunting bacterial and fungal membrane permeability is an efficient way to kill prokaryonts; this has been shown with pore formers such as amphotericin B and filimarisine (also called filipin). Amphotericin B and filimarisine are cyclic polyene antifungal drugs that interact with membrane sterols and create pores through which ions leak.[50,51] Valinomycin is also a cyclic (nonpolyenic) compound with high specificity as K^+ carrier in prokaryonts and eukaryontsl; it does not form pores but also enables the diffusion of K^+ through the membrane:[52]

> "It takes a membrane to make sense out of disorder in biology. To stay alive you have to be able to hold out against equilibrium, maintain imbalance, bank against entropy, and you can only transact this business with membranes in our kind of world."
>
> Lewis Thomas.[53] Cited by Harold.[54]

Thus, it is not surprising that altering cell membrane permeability to ions of almost any kind should be a very efficient way to kill organisms, such as prokaryonts, living in extreme conditions where the external medium is usually extremely variable and anisosmotic with cell plasma. With the present evidence it is not possible to know exactly which of the mechanisms described above is involved in the fungicidal effect of *T. discrepans* venom peptides. Yet, scorpion venom peptides of >3 kDa are generally globular with cysteine-rich disulfide bridges. To our knowledge, none of these globular proteins has ever been shown to be a channel former or an ion carrier through plasmatic membranes. There is ample evidence suggesting that scorpion venom peptides interact with membrane receptors and open or block preexisting ionic channels.[3,33,55−57] Thus, the effect of *T. discrepans* venom peptides on Na−CoroNa Red outflow from *M. phaseolina* is strongly suggestive of a conductance, of unknown selectivity, which lets Na^+ outflow from the hyphae.

Sterol composition of plasmatic membranes is critical for membrane fluidity, and membrane fluidity is in turn critical for the proper function of transmembrane molecules, such as ionic channels. One of the most effective groups of clinical and agricultural antifungals are triazoles.[58−60] Triazoles act by disrupting the close packing of acyl chains of phospholipids, impairing the functions of certain membrane-bound enzyme systems such as ATPase and enzymes of the electron transport system, thus inhibiting fungus growth. They do this by blocking the synthesis of ergosterol (ergosta-5,7,22-trien-3β-ol), by inhibiting the enzyme lanosterol 14α-demethylase, and by accumulation of methylated sterol precursors.[58] Ergosterol is present in fungal cell membranes, and its synthesis is targeted by many pharmaceutical and agrochemical fungicides. Ergosterol is also present in the cell membranes of some protists, such as trypanosomes.[61] This is the basis for the use of some antifungals against West African sleeping sickness. Miconazole, itraconazole, and clotrimazole work in a different way, inhibiting synthesis of ergosterol from lanosterol. Ergosterol is a smaller molecule than

lanosterol; it is synthesized by combining two molecules of farnesyl pyrophosphate, a 15-carbon-long terpenoid, into lanosterol, which has 30 carbons. Then, two methyl groups are removed, making ergosterol.

Studies of sterols in the Basidiomycota genus *Ganoderma* have shown that the most interesting secondary sterol metabolites are derivatives from ergostane, lanostane, and lanostanic acid;[62] the most abundant sterols in *Ganoderma lucidum* are ergosterol, which has been reported at concentrations of 0.3−0.4%, and also ergosta-5,7-dien-3β-ol (dihidroergosterol), ergosta-7-en-3β-ol, ergosta-5,7,9(11),22-tetraen-3-ol, and ergosteril peroxide. Studies in *Laccaria laccata*, another Basidiomycota, have identified ergosterol, ergosta-7,22-dien-3β-ol, ergosta-7-en-3β-ol, ergosta-5,7,9(11),22-tetraen-3β-ol, and stigmast-5-en-3β-ol.[63] Yet, our work seems to be the first sterol composition study of *M. phaseolina* or of any other similar pathogenic fungus. We have found that the only sterol constituting *M. phaseolina* membrane is ergosterol. Our work indicates that the synthesis of ergosterol was partially blocked in *M. phaseolina* after exposure to **F5**. This peptide blocked the sterol route and induced accumulation of squalene, an ergosterol precursor. This suggested a possible inhibition of enzymes as squalene epoxidase or lanosterol cyclase and should be indicative of an action mechanism similar to the triazoles. Furthermore, **F1**, **F6**, and **F7** induced fungal structural sterol changes by replacing ergosterol by structurally similar sterols such as desmosterol, β-sitosterol, or 22,23-dihydrostigmasterol. In fungal cell membranes, ergosterol has the same role as cholesterol in animal cells. The possibility exists that the mechanism of action of **F5** is similar to that of triazol antimicotics, resulting in an inhibition of the biosynthesis of sterols at squalene level; it is also possible that these scorpion toxins interact directly with membrane ergosterol.

The antifungal toxins isolated from *T. discrepans* scorpion venom seemingly altered *M. phaseolina* viability through three different ways: inhibiting fungus esterases, altering Na^+ membrane permeability, and inhibiting ergosterol synthesis or replacing it by other membrane sterols. **F7** induced the most potent antifungal effect with a MIC of 0.4 μg/μL and an IC_{50} of 0.13 μg/μL. The action of these toxins on fungal sterol composition also poses questions on the mechanism to induce changes on Na^+ membrane permeability discussed above. Membrane sterols are crucial to keep the proper membrane fluidity. Whereas sterols add firmness and integrity to the plasma membrane and prevent it from becoming overly fluid, they also help to maintain its fluidity. At the high concentrations found in plasma membranes (close to 50%, molecule for molecule), sterols help to separate the phospholipids so that the fatty acid chains cannot come together and crystallize. Therefore, sterols prevent fluidity extremes in the cell membrane.[64,65] Reductions in membrane fluidity such as the one produced by low temperatures and by replacement of water by heavy water (D_2O) reduce membrane fluidity and slow or block ionic activity.[66−71] Moreover, increasing the fluidity of the membrane of a squid giant axon by heating it 10−15 °C above its physiological temperature reversibly depolarizes its plasmatic membrane and makes it leaky to ion channels.[70] It thus seems that interfering with sterol synthesis is an important mechanism behind the effect of the antifungal *T. discrepans* venom components described here. However, the antifungal effects at short times are indicative of a direct esterase inhibition, which, with the increased membrane leakiness to Na^+, makes the fungus inviable. If there is more than one direct effect of a fungicide, the speed of evolution of resistance to it may be greatly reduced. An outstanding feature of the toxins isolated in this work is that they seem to attack simultaneously two or more targets fundamental for *M. phaseolina* survival.

AUTHOR INFORMATION

Corresponding Author

*E-mail: gina.dsuze@gmail.com.

Funding Sources

This research was partially supported by Laboratorios Silanes/Instituto Bioclón, Mexico, by Venezuelan FONACIT Grant S1-2001000908 (G.D'S.), by a FONACIT grant to IVIC's Project 416 (G.D'S.), by the Brazilian Conselho Nacional de Desenvolvimento Cientifico e Tecnologico (CNPq) (J.P.), by Fundação de Amparo a Pesquisa, Rio de Janeiro (FAPERJ), and by Fundação Oswaldo Cruz/PDTIS, Brazil (J.P.).

ACKNOWLEDGMENT

We are indebted to the people of San Antonio de Los Altos and their Fire Department for the supply of the scorpions. We greatly appreciate the technical assistance of Moisés Sandoval (CBB), Rosa Martínez (CBB), Álvaro Álvarez (Chemistry Center), and Yelitza Díaz (Chemistry Analysis Services). Also, we are grateful to Drs. María González (INIA) and Luís Subero (UCV) for the identification and supply of fungi. We greatly appreciate the comments of an unknown reviewer, which led to the improvement of the last paragraph of the Discussion.

REFERENCES

(1) Knogge, W. Fungal infection of plants. *Plant Cell* **1996**, *8*, 1711–1722.

(2) Fontecilla-Camps, J. C. Three-dimensional model of the insect-directed scorpion toxin from *Androctonus australis* Hector and its implication for the evolution of scorpion toxins in general. *J. Mol. Evol.* **1989**, *29*, 63–67.

(3) Rodriguez de la Vega, R. C.; Possani, L. D. Overview of scorpion toxins specific for Na^+ channels and related peptides: biodiversity, structure−function relationships and evolution. *Toxicon* **2005**, *46*, 831–844.

(4) Cociancich, S.; Goyffon, M.; Bontems, F.; Bulet, P.; Bouet, F.; Menez, A. Purification and characterization of a scorpion defensin, a 4 kDa antibacterial peptide presenting structural similarities with insect defensins and scorpion toxins. *Biochem. Biophys. Res. Commun.* **1993**, *194*, 17–22.

(5) Torres-Larios, A.; Gurrola, G. B.; Zamudio, F. Z.; Possani, L. D. Hadrurin, a new antimicrobial peptide from the venom of the scorpion *Hadrurus aztecus*. *Eur. J. Biochem.* **2000**, *267*, 5023–5031.

(6) Ehret-Sabatier, L.; Loew, D.; Goyon, M.; Fehlbaum, P.; Homann, J. A.; Van Dorsselaer, A.; Bulet, P. Characterization of novel cysteine-rich antimicrobial peptides from scorpion blood. *J. Biol. Chem.* **1996**, *271*, 29537–29544.

(7) Conde, R.; Zamudio, F. Z.; Rodriguez, M. H.; Possani, L. D. Scorpine, an anti-malaria and anti-bacterial agent purified from scorpion venom. *FEBS Lett.* **2000**, *471*, 165–168.

(8) Corzo, G.; Escoubas, P.; Villegas, E.; Barnham, K. J.; He, W.; Norton, R.; Nakajima, T. Characterization of unique amphipathic antimicrobial peptides from venom of the scorpion *Pandinus imperator*. *Biochem. J.* **2001**, *359*, 35–45.

(9) Uawonggul, N.; Thammasirirak, S.; Chaveerach, A.; Arkaravichien, T.; Bunyatratchata, W.; Ruangjirachuporn, W.; Jearranaiprepame, P.; Nakamura, T.; Matsuda, M.; Kobayashi, M.; Hattori, S.; Daduang, S. Purification and characterization of heteroscorpine-1 (HS-1) toxin from *Heterometrus laoticus* scorpion venom. *Toxicon* **2007**, *49*, 19–29.

(10) Díaz, P.; D'Suze, G.; Salazar, V.; Sevcik, C.; Shannon, J. D.; Sherman, N. E.; Fox, J. W. Antibacterial activity of six novel peptides

from *Tityus discrepans* scorpion venom. a fluorescent probe study of microbial membrane Na^+ permeability changes. *Toxicon* **2009**, *54*, 802–817.

(11) Bulet, P.; Stöcklin, R.; Menin, L. Anti-microbial peptides: from invertebrates to vertebrates. *Immunol. Rev.* **2004**, *198*, 169–184.

(12) Pimenta, A. M.; Stöcklin, R.; Favreau, P.; Bougis, P. E.; Martin-Eauclaire, M. F. Moving pieces in a proteomic puzzle: mass fingerprinting of toxic fractions from the venom of *Tityus serrulatus* (Scorpiones, Buthidae). *Rapid Commun. Mass Spectrom.* **2001**, *15*, 1562–1572.

(13) Batista, C. V. F.; D'Suze, G.; Gomez-Lagunas, F.; Zamudio, F. Z.; Encarnación, S.; Sevcik, C.; Possani, L. D. Proteomic analysis of *Tityus discrepans* scorpion venom and amino acid sequence of novel toxins. *Proteomics* **2006**, *6*, 3718–3727.

(14) D'Suze, G.; Zamudio, F. Z.; Gomez-Laguna, F.; Possani, L. D. A novel K^+ channel blocking toxin from *Tityus discrepans* scorpion venom. *FEBS Lett.* **1999**, *456*, 146–148.

(15) Simpson, R. J. Peptide mapping and sequence analysis of gel-resolved proteins. In *Proteins and Proteomics: a Laboratory Manual*; Simpson, R. J., Ed.; Cold Spring Harbor Laboratory: Cold Spring Harbor, NY, 2003; pp 343−424.

(16) Broekaert, W.; Terras, F.; Cammue, B.; Banderleyden, J. An automated quantitative assay for fungal growth inhibition. *FEMS Microbiol. Lett.* **1990**, *69*, 55–60.

(17) Ludwig, A.; Boller, T. A method for the study of fungal growth inhibition by plant proteins. *FEMS Microbiol. Lett.* **1990**, *69*, 61–66.

(18) NCCLS (National Committee for Clinical Laboratory Standards). Reference method for broth dilution antifungal susceptibility testing of filamentous fungi, approved standard. *NCCLS Document M38-A*; 2002; Vol. *22*, pp 1−29.

(19) Dittmer, U.; Weltzien, H. C. A rapid viability test for sclerotia with fluorescein diacetate. *J. Phytopathol.* **1990**, *130*, 59–64.

(20) Guilbault, G. G.; Kramer, D. N. New direct fluorometric method for measuring dehydrogenase activity. *Anal. Chem.* **1994**, *36*, 2497–2498.

(21) Monheit, J. G.; Brown, G.; Kott, M. M.; Schmidt, W. A.; Moore, D. G. Calcofluor white detection of fungi in cytopathology. *Am. J. Clin. Pathol.* **1986**, *85*, 222–225.

(22) Baron, S.; Caplanusi, A.; Van de Ven, M.; Radu, M.; Despa, S.; Lambrichts, I.; Ameloot, M.; Steels, P.; Smets, I. Role of mitochondrial Na^+ concentration, measured by CoroNa Red, in the protection of metabolically inhibited MDCK cells. *J. Am. Soc. Nephrol.* **2005**, *16*, 3490–3497.

(23) Bernardinelli, Y.; Azarias, G.; Chatton, J. Y. *In situ* fluorescence imaging of glutamate-evoked mitochondrial Na^+ responses in astrocytes. *Glia* **2006**, *54*, 460–470.

(24) Iwamoto, M.; Allen, R. D. Uptake and rapid transfer of fluorescent ceramide analogues to acidosomes (late endosomes) in *Paramecium*. *J. Histochem. Cytochem.* **2004**, *52*, 555–565.

(25) Ahn, A. H.; Basbaum, A. I. Tissue injury regulates serotonin 1d receptor expression: implications for the control of migraine and inflammatory pain. *J. Neurosci.* **2006**, *26*, 8332–8338.

(26) Bligh, E. G.; Dyer, W. J. A rapid method of total lipid extraction and purification. *Can. J. Physiol. Pharmacol.* **1959**, *37*, 911–917.

(27) Visbal, G.; San-Blas, G.; Murgich, J.; Franco, H. *Paracoccidioides brasiliensis*, paracoccidioidomycosis, and antifungal antibiotics. *Curr. Drug Targets−Infect. Dis.* **2005**, *5*, 211–226.

(28) Hollander, M.; Wolfe, D. A. *Nonparametric Statistical Procedures*; Wiley: New York, 1973.

(29) Brazón, J.; D'Suze, G.; D'Errico, M. L.; Sevcik, C.; Arocha-Piñango, C. L.; Guerrero, B. Discreplasminin, a plasmin inhibitor isolated from *Tityus discrepans* scorpion venom. *Arch. Toxicol.* **2009**, *83*, 669–678.

(30) D'Suze, G.; Batista, C. V. F.; Frau, A.; Murgia, A. R.; Zamudio, F. Z.; Sevcik, C.; Possani, L. D. Discrepin, a new peptide of the subfamily a-ktx15, isolated from the scorpion *Tityus discrepans* irreversibly blocks K^+-channels (IA currents) of cerebellum granular cells. *Arch. Biochem. Biophys.* **2004**, *43*, 256–263.

(31) D'Suze, G.; Corona, F.; Possani, L. D.; Sevcik, C. High performance liquid chromatography purification and amino acid sequence of toxins from the muscarinic fraction of *Tityus discrepans* scorpions venom. *Toxicon* **1996**, *34*, 591–598.

(32) D'Suze, G.; Sevcik, C.; Corona, M.; Zamudio, F. Z.; Batista, C. V. F.; Coronas, F. I.; Possani, L. D. Ardiscretin a novel arthropselective toxin from *Tityus discrepans* scorpion venom. *Toxicon* **2004**, *43*, 263–272.

(33) D'Suze, G.; Sevcik, C.; Perez, J. F.; Fox, J. W. Isolation and characterization of a potent curarizing polypeptide from *Tityus discrepans* scorpion venom. *Toxicon* **1997**, *35*, 1683–1689.

(34) Brazón, J.; Guerrero, B.; Arocha-Piñango, C. L.; Sevcik, C.; D'Suze, G. Efecto del veneno del escorpión *Tityus discrepans* sobre el tiempo de protrombina, el tiempo de tromboplastina parcial y su actividad coagulante directa en plasma humano o fibrinógeno purificado. *Invest. Clin.* **2008**, *49*, 49–58.

(35) Borges, A.; García, C.; Lugo, E.; Alfonzo, M. J.; Jowers, M. J.; Op den Camp, H. Diversity of long-chain toxins in *Tityus zulianus* and *Tityus discrepans* venoms (Scorpiones, Buthidae): molecular, immunological, and mass spectral analyses. *Comp. Biochem. Physiol. C: Toxicol. Pharmacol.* **2006**, *142*, 240–252.

(36) Diego-Garcia, E.; Batista, C. V. F.; Garcia-Gomez, B. I.; Lucas, S.; Candido, D. M.; Gomez-Lagunas, F.; Possani, L. D. The Brazilian scorpion *Tityus costatus* Karsch: genes, peptides and function. *Toxicon* **2005**, *45*, 273–283.

(37) DSuze, G.; Schwartz, E. F.; García, B. I.; Sevcik, C.; Possani, L. D. Molecular cloning and nucleotide sequence analysis of genes from *Tityus discrepans* cDNA library. *Biochemie* **2009**, *91*, 1010–1019.

(38) Stubberfield, L. C. F.; Shaw, P. J. A. A comparison of tetrazolium reduction and FDA hydrolysis with other measurements of microbial activity. *J. Microbiol. Methods* **1990**, *12*, 151–162.

(39) Kramer, D. N.; Guilbault, G. G. A substrate for the fluorometric determination of lipase activity. *Anal. Chem.* **1963**, *35*, 588.

(40) Thevissen, K.; Terras, F. R. G.; Broekaert, W. F. Permeabilization of fungal membranes by plant defensins inhibits fungal growth. *Appl. Environ. Microbiol.* **1999**, *65*, 5451–5458.

(41) Gustin, M. C.; Zhou, X. L.; Martinac, B.; Kung, C. A mechanosensitive ion channel in the yeast plasma membrane. *Science* **1988**, *242*, 762–765.

(42) Salyman, L. Electrical properties of *Neurospora crassa*. Respiration and the intracellular potential. *J. Gen. Physiol.* **1965**, *49*, 93–116.

(43) Clifford, L. L.; Slayman, L.; Longa, W. S.; Gradmann, D. Action potentials in *Neurospora crassa*, a mycelial fungus. *Biochim. Biophys. Acta* **1976**, *4*, 732–744.

(44) Zhou, X. L.; Kung, C. A mechanosensitive ion channel in *Schizosaccharomyces pombe*. *EMBO J.* **1992**, *11*, 2869–2875.

(45) Zhou, X. L.; Stumpf, M. A.; Hoch, H. C.; Kung, C. A mechanosensitive channel in whole cells and in membrane patches of the fungus *Uromyces*. *Science* **1991**, *253*, 1415–1417.

(46) Martinac, B.; Saimi, Y.; Kung, C. Ion channels in microbes. *Physiol. Rev.* **2008**, *88*, 1449–1490.

(47) Huang, M. E.; Chuat, J. C.; Galibert, F. A voltage-gated chloride channel in the yeast *Saccharomyces cerevisiae*. *J. Mol. Biol.* **1994**, *242*, 595–598.

(48) Clapham, D. E. TRP channels as cellular sensors. *Nature* **2003**, *426*, 517–524.

(49) Ren, D.; Navarro, B.; Xu, H.; Yue, L.; Shi, Q.; Clapham, D. E. A prokaryotic voltage-gated sodium channel. *Science* **2001**, *294*, 2372–2375.

(50) Hamilton-Miller, J. M. T. Chemistry and biology of the polyene macrolide antibiotics. *Bacteriol. Rev.* **1973**, *27*, 166–196.

(51) Ellis, D. Amphotericin B: spectrum and resistance. *J. Antimicrob. Chemother.* **2002**, *49*, 7–10.

(52) Huang, H. W.; Williams, C. R. Structure of valinomycin−K^+ complex in solution by extended x-ray absorption fine structure. *Biophys. J.* **1981**, *33*, 269–273.

(53) Thomas, L. *The Lives of a Cell: Notes of a Biology Watcher*; Viking Press, Penguin Books, 1974.

(54) Harold, F. M. Ion currents and physiological functions in microorganisms. *Annu. Rev. Microbiol.* **1977**, *31*, 181–203.

(55) Giangiacomo, K. M.; Sugg, E. E.; Garcia-Calvo, M.; Leonard, R. J.; McManus, O. B.; Kaczorowski, G. J.; Garcia, M. L. Synthetic charybdotoxin−iberiotoxin chimeric peptides define toxin binding sites on calcium-activated and voltage-dependent potassium channels. *Biochemistry* **1993**, *32*, 2363–2370.

(56) DeBin, J. A.; Strichartz, G. R. Chloride channel inhibition by the venom of the scorpion *Leiurus quinquestriatus*. *Toxicon* **1991**, *29*, 1403–1408.

(57) Rodriguez de la Vega, R. C.; Possani, L. D. Current views on scorpion toxins specific for K^+-channels. *Toxicon* **2004**, *43*, 865–875.

(58) Brunton, L.; Lazo, J.; Parker, K. Antimicrobial agents: antifungal agents. In *Goodman and Gilman's The Pharmacological Basis of Therapeutics*, 11th ed.; McGraw-Hill: San Francisco, CA, 2006; Chapter 48.

(59) Klix, M. B.; Verreet, J.-A.; Beyer, M. Comparison of the declining triazole sensitivity of *Gibberella zea*e and increased sensitivity achieved by advances in triazole fungicide development. *Crop Prot.* **2007**, *26*, 683–690.

(60) Klittich, C. J. Milestones in fungicide discovery: chemistry that changed agriculture. *Plant Health Progr.* **2008**, doi: 10.1094/PHP-2008-0418-01-RV (http://www.plantmanagementnetwork.org/pub/php/review/2008/milestones/).

(61) Roberts, C. W.; McLeod, R.; Rice, D. W.; Ginger, M.; Chance, M. L.; Goad, L. J. Fatty acid and sterol metabolism: potential antimicrobial targets in apicomplexan and trypanosomatid parasitic protozoa. *Mol. Biochem. Parasitol.* **2003**, *126*, 129–142.

(62) Nishitoba, T.; Sato, H.; Shirasu, S.; Sakamura, S. Evidence on the strain-specific terpenoid pattern of *Ganoderma lucidum*. *Agric. Biol. Chem.* **1986**, *50*, 2151–2154.

(63) Nieto, R.; Ivonne, J.; Cucaita, V.; Edna, P. Fatty acids, esters and sterols of the *Laccaria laccata* mushroom. *Rev. Colomb. Quim.* **2007**, *36*, 277–284.

(64) Cooper, R. A. Influence of increased membrane cholesterol on membrane fluidity and cell function in human red blood cells. *J. Supramol. Struct.* **1978**, *8*, 413–430.

(65) Alberts, B.; Johnson, A.; Lewis, J.; Raff, M.; Roberts, K.; Walter, P. *Molecular Biology of the Cell*, 4th ed.; Garland Science, Taylor & Francis Group: New York, 2002.

(66) Barnes, T. C. The influence of heavy water and temperature on the electrical potential of frog skin. *J. Cell. Comp. Phys.* **1939**, *13*, 39–50.

(67) Kaminer, B.; Kimura, J. Deuterium oxide: inhibition of calcium release in muscle. *Science* **1972**, *176*, 406–407.

(68) Huxtable, R.; Bressler, R. The effect of deuterium ion concentration on the properties of sarcoplasmic reticulum. *J. Membr. Biol.* **1974**, *17*, 189–197.

(69) Schauf, C. L.; Bullock, J. O. Modifications of sodium channel gating in *Myxicola* giant axons by deuterium oxide, temperature, and internal cations. *Biophys. J.* **1979**, *27*, 193–208.

(70) Sevcik, C. Temperature dependence of tetrodotoxin effect in squid giant axons. *J. Physiol.* **1982**, *325*, 187–194.

(71) Tillman, T. S.; Cascio, M. Effects of membrane lipids on ion channel structure and function. *Cell Biochem. Biophys.* **2003**, *38*, 161–190.